
Deep Curiosity Loops in Social Environments

Jonatan Barkan
 Curiosity Lab,
 Department of Industrial Engineering
 Tel-Aviv University, Israel
 jbarkan14@gmail.com

Goren Gordon
 Curiosity Lab,
 Department of Industrial Engineering
 Tel-Aviv University, Israel
 goren@gorengordon.com

Abstract

Inspired by infants' intrinsic motivation to learn, which values informative sensory channels contingent on their immediate social environment, we developed a deep curiosity loop (DCL) architecture. The DCL is composed of a learner, which attempts to learn a forward model of the agent's state-action transition, and a novel reinforcement-learning (RL) component, namely, an Action-Convolution Deep Q-Network, which uses the learner's prediction error as reward. The environment for our agent is composed of visual social scenes, composed of sitcom video streams, thereby both the learner and the RL are constructed as deep convolutional neural networks. The agent's learner learns to predict the zero-th order of the dynamics of visual scenes, resulting in intrinsic rewards proportional to changes within its social environment. The sources of these socially informative changes within the sitcom are predominantly motions of faces and hands, leading to the unsupervised curiosity-based learning of social interaction features. The face and hand detection is represented by the value function and the social interaction optical-flow is represented by the policy. Our results suggest that face and hand detection are emergent properties of curiosity-based learning embedded in social environments.

1 Introduction

Infants are masters of learning, as they assimilate vast amounts of novel stimuli through their active interaction with their environment. Moreover, babies have an intrinsic motivation to learn and attend to the most informative channels available to them. This curiosity drive is the hallmark of young children's behavior. On the other hand, infants do not have full control over their surrounding, as locomotion comes much later in development. Hence, the visual scenarios infants are embedded in is dictated by their caregivers, which in turn dominate the visual stimuli. In other words, infants' visual scenarios are mostly composed of other social agents interacting with them [7].

The combination of the curiosity drive and visual social scenarios, found in infants, guided our novel Deep Curiosity Loop (DCL) architecture. Artificial curiosity concerns with intrinsic motivation in the field of reinforcement learning (RL) wherein the reward is intrinsic to the agent, as opposed to extrinsically given by the experimenter [29, 25, 24]. The reward represents some form of learning or learning progress, quantified by e.g. prediction error, reduction in prediction error, surprise, empowerment, etc. [21]. The curiosity loop is hence composed of a learner, which attempts to learn sensorimotor correlations, e.g. the forward model of the agent's interaction with its environment, and an RL component which receives the intrinsic reward, thereby resulting in a behavior that attempts to optimize the learning process (of the learner) [10]. In our Deep Curiosity Loop architecture, due to the visual and temporal stream of information, the learner is a deep convolutional neural network that attempts to learn the (actionable) dynamics of visual scenes. The RL component is constructed as an

action-convolution deep-Q network (AC-DQN), wherein an action is learned *for each pixel in the video stream*.

Mimicking infants’ visual environment, we take as training data visual social scenarios, i.e. sitcom videos. In these videos, the dominant activity is performed by social agents. Combining these scenarios with the DCL architecture, we hypothesize that the agent will attempt to learn the dynamics of the video (learner) and hence will learn to attend, i.e. predict high value and select actions towards (AC-DQN), the most informative or surprising parts of the scene. We hypothesize that faces are these most informative parts and confirm this hypothesis from our data, whereas hands are also a dominant social communication channel. This results in the unsupervised (curiosity-based) learning of a value function that represents Socially-relevant Feature Detection (SFD), namely, face and hand detection, i.e. high value for faces and hands due to their informative nature, and a social interaction-optical flow, i.e. local actions converging to the social features in the scene as learned by the AC-DQN.

The main contributions of this paper are threefold: (i) a novel deep curiosity loop architecture, that combines CNN with intrinsic reward and DQN; (ii) a unique RL algorithm, i.e. action-convolution DQN that enables a highly parallelized RL scheme with “passive” video stream and; (iii) an unsupervised learning of face and hand detection.

2 Motivation and Related Works

Previous studies have shown that human babies are able to see in the first few months of their life [4] as well as to detect and recognize faces ([13]). First Jayaraman et al. [14] and later Fausey et al. [7] proved that in the first year of life the relevant environment has a distribution with disproportionately high probability to contain faces. They revealed this lopsidedness decreases as the year progresses and is replaced by another non-uniform distribution with a disproportionate amount of moving hands, often attached to objects, as it pushes into its second year.

Curiosity has been described as a predominant driver of human behavior and it had not gone unnoticed by the Artificial Intelligence community [29, 30]. The re-emerging field is highly related to developmental robotics, which is the interdisciplinary field that attempts to integrate developmental psychology, machine learning and robotics, by studying infant’s learning behavior and implementing those insights in robots that learn by themselves [28, 18, 25, 1, 40, 5]. This framework focuses on intrinsic motivation [25, 1, 32, 16, 31], where the reward of the agent does not come from an outside source but rather from internal processing. Thus, Artificial curiosity (AC) [28, 18, 25, 1, 40] was inspired by developmental psychology and attempted to create a curious robot, where curiosity is often defined as “behavior driven by learning” [11, 9]. By rewarding the learning progress, which can be computed in several different ways [21], and using reinforcement learning (RL) algorithms [34] one can adapt the behavior so as to optimize the learning process.

One of the possible intrinsic reward functions is the history-agnostic prediction error of an internal model. Gordon and Ahissar [10] introduced the notion of Hierarchical Curiosity Loops (HCL), an architecture whereby each loop selects the optimal action that maximizes an agent’s learning of sensory-motor correlations. The intrinsic reward was produced by a learning object internal to the agent, namely a Learner, presented with the task of modeling the sensory-motor internal models, e.g. forward model, which means taking the current state and action of the agent and predicting the next state.

It has been shown that this framework can create emerging exploratory behavior, such as the emergent appearance of proximo-distal maturation from purely intrinsic motivation [33], in addition to complex arena-exploration motor primitives [12]. Many interesting results have come from this field back into Neuroscience, attempting to explain specific developmental phenomena by observing them in robots [9, 33, 23]. Accordingly, the same framework has been suggested to give plausible explanation to animals’ exploration, e.g. vibrissae movement and locomotive exploration in rodents [11, 12], as well as infants’ behaviors, such as the order of phonetic learning [23] and hand-eye coordinated movements [9]. While these examples differ slightly in their instantiation of the curiosity-based algorithm, they mostly differ in the environment the agent is embedded in.

In this work we wanted to simulate a similar environment to that of an infant in order to check our hypothesis that socially relevant features detection can be learned without preexisting knowledge and

by using curiosity alone. In effect, we hypothesize the correctness of the equation:

$$\begin{array}{ccccc} \text{Social Environment} & + & \text{Curiosity} & = & \text{Social Interaction Detector} \\ (\text{faces and hands}=\text{information}) & & (\text{information}=\text{value}) & & (\text{face \& hand detector}) \end{array} \quad (1)$$

The literature regarding social features detection is composed of two venues, namely, face detection and image segmentation. Two main approaches to face detection currently dominate the field. The first is by feature selection following the seminal work of Viola and Jones [36] [38], the industry’s benchmark due to its implantations in many popular libraries (such as OpenCV). Their face detection algorithm produces templates for faces by learning to select profitable features and training a classifier with them on a labeled dataset. It was the first to perform online inference rapidly. To its detriment, small differences in the same object necessitates specialized templates, most notably frontal and profile faces. This is due to susceptibility to non-symmetry (monotonicity) and extreme light conditions among others ([20], [8, 41] respectively).

The second approach is by way of Deep Learning methods, primarily Deep Convolutional Neural Networks (DCNN). In contrast with the previous framework, here the features are generated automatically and with respect to the data they are trained on. It has no a-priori knowledge about the features nor the areas it should prioritize to find patterns. Of these methods, the technique of using a region proposal network to suggest possible regions with faces is at the heart of many current state of the art methods, currently led by Jiang and Learned-Miller [15] who employ the Faster R-CNN [26] method. Both techniques lie in the realm of supervised learning, as they are provided with a set of positive and negative examples.

As for the unsupervised case, there has not been many successful attempts. Le [19] seminal work proved face detecting features, among others, can be learned with a Deep Autoencoder. Yet they did not arrive at a face detection model and had to measure each feature’s performance in classifying faces. Furthermore, their network used 1 billion parameters and trained on 10 million images. A somewhat recent work by Walther and Würtz [39], aimed for the purpose of unsupervised face detection, has managed to perform well by leveraging Organic Computing. However, it has not been tested on real-world data and its processing time for a single image is close to 1 minute.

Regarding image segmentation, Long et al. [22] trained a fully convolutional network for image segmentation. While not focusing on socially relevant features exclusively, these were part of the labeled training set for the supervised learning procedure. The trained network and its adaptation were used in socially-specific scenarios in Ben-Yosef et al. [2] in order to detect social interaction in still images. However, all these attempts used fully labeled supervised learning algorithms.

3 Model

In this section we present our proposed architecture and its embedding environment. The environment is a generator of RGB images that may come from a single robot’s camera or another continuous video feed. Thus the images are successive in time. For this experiment, all images are of fixed height h and width w and have RGB channels. The state space S is defined as the set of all possible images. We constrain the action space A to movement parallel to the axes and to a single step size. As a result, the possible actions we allow are staying in the same location (using the sign \circ) or moving k pixels up (\uparrow_k), down (\downarrow_k) left (\leftarrow_k) or right (\rightarrow_k), with a fixed step size k .

In order to capitalize off of every single image, we introduce a novel approach which parallelize the agent’s curiosity loop, surveying all potential states collectively. We do this with the simple trick of convolution, made possible by using Deep Convolutional Neural Networks (DCNN’s) as the learning algorithms of the leaning elements of the Deep Curiosity Loop. With this in mind we define the state space \mathbb{S} as the set of all possible bounding boxes with predetermined n and m as height and width respectively, whereas the action space \mathbb{A} becomes the set of matrices with entries from $\{\circ, \uparrow_k, \downarrow_k, \leftarrow_k, \rightarrow_k\}$. We also add for notation $\hat{\mathbb{A}}$ as the one-hot representation of an action matrix \mathbb{A} the new action space.

3.1 Learner

Our Learner Φ^L is a mapping that aims to learn a forward model of the agent’s state-action transition. We chose a convolutional neural network with a single layer, without pooling and with a ReLU

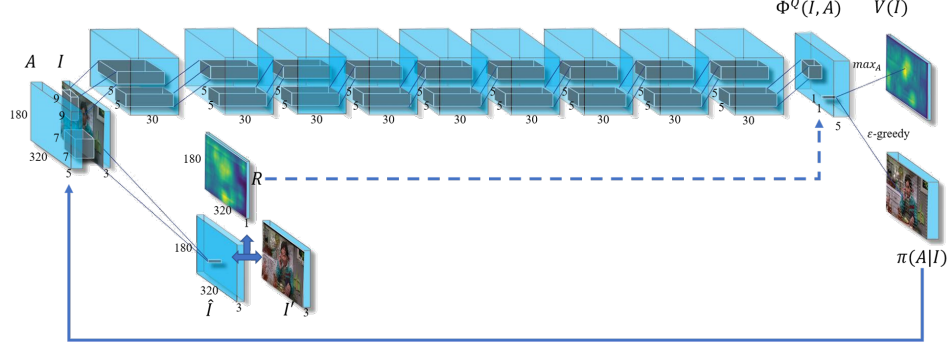


Figure 1: The Deep Curiosity Loops architecture.

activation, that takes as input an image $I \in S$ and a one-hot encoding of an action, $\hat{\mathbf{A}} \in \hat{\mathbb{A}}$ and outputs a predicted $\hat{I} \in S$, $\Phi^L(I, \hat{\mathbf{A}}) \mapsto \hat{I}$. Given the next image $I' \in S$ the learner's cost function, J^L is given by the Mean Squared Error between \hat{I} and I' .

$$J_L(I, \hat{\mathbf{A}}, I') = \frac{1}{3wh} \sum_{i,j,c} \left(\Phi^L(I, \hat{\mathbf{A}})[i, j, c] - I'[i, j, c] \right)^2 \quad (2)$$

It updates by Stochastic Gradient Descent with momentum [3]. Since this is a pure convolutional network, the output (image) is the same size as the input (image), wherein each pixel in the output is affected by $n \times m$ pixels in the input image, centered on it.

3.2 Intrinsic Rewards Image

In order to compute the reward we decompose its calculation to two parts. Instead of using the learner's loss directly, we devised a slightly different reward function. First we compute the mean squared difference with respect to each pixel's maximum color value. This results in an image-like value structure with the same dimensions as the input image. Second, we convolve the result with an averaging filter with the same dimensions and zero-padding such that it retains its size. This has the desired affect of averaging with respect to the receptive field of the AC-DQN (see below). This too results in an image-like 2d (no depth/color, or depth 1) structure where every pixel value represents the reward of the state that this pixel represents.

$$\mathbf{R}(I, \hat{\mathbf{A}}, I') = \frac{1}{wh} \sum_{i,j} \left(\max_c \Phi^L(I, \hat{\mathbf{A}})[i, j, c] - \max_c I'[i, j, c] \right)^2 \quad (3)$$

3.3 Action-Convolution Deep-Q Network

With the intention of parallelizing the Deep Curiosity Loop we devised a new algorithm called Action-Convolution Deep-Q Network (AC-DQN). It is a variant of Deep Q-Network (DQN) and Double Deep Q-Network (DDQN). These networks are essentially Q function approximators that employ the Deep CNN structure and learn through gradient descent (ADAM [17]) to minimize the TD-error. As with both algorithms, we make use of Experience Replay (prioritize [27]). Between layers we use instance normalization [35] which does not require turning off after learning.

AC-DQN is a deep CNN architecture Φ^Q with an image as its input and a matrix with the same height h and width w as the reward. The network's last layer is of dimensions $h \times w \times |A|$, where A is the action space. We are using DDQN, hence the target \mathbf{T} is the matrix-addition of the reward matrix ("image") and the discounted approximation of the output of Φ^Q on the next frame, and the TD-error is denoted as δ .

$$\mathbf{T} = \mathbf{R} + \gamma \cdot \max_{\hat{\mathbf{A}} \in \hat{\mathbb{A}}} \Phi^Q(I', \hat{\mathbf{A}}) \quad \delta = |\Phi^Q(I, \hat{\mathbf{A}}) - T| \quad (4)$$

The final AC-DQN version uses a DCNN with 10 convolutional layers. Each hidden layer has a filter depth of 30 with ReLU activations whereas the output layer has depth 5 to match the number of actions. This layer has a linear activation function. Each layer’s filter dimensions is 5×5 except the first for which is 9×9 . Effectively, the AC-DQN has a receptive field of 45×45 with respect to the input layer.

The novelty of our proposed AC-DQN architecture is in its output layer. In traditional in DQN variants, given input s , the output of the network is a vector where the entry for each action a represents the prediction of $Q(s, a)$. However, in order to parallelize the Deep Curiosity Loop our AC-DQN’s output is a matrix with the height and width of the input image I and with depth the size of the action space (here $|A| = 5$). In essence, we compute the Q-value for *each pixel* (environment) in the input image. Consequently, AC-DQN’s loss function is actually the mean of the TD-error over all pixels.

4 Experiments

4.1 Data

The original dataset consists of 10 seasons of the hit Television series The Big Bang Theory as our “social visual scene”, most consisting of 24 episodes. Below we describe the preprocessing and the reasoning behind it.

Contrary to traditional DL training, we attempt to mimic infants’ environment and processing. Hence, we use *online learning* and consider only actions *within* the image. The latter model eye movement as changing the center of the “visible image”, whereas head shifts can be seen as corresponding to camera movement. For this reason we divided each episode into shots, each with a minimal movement of the camera. We have done so by upholding a threshold for the maximal amount of pixel turnover rate on the outskirts of the frames. We selected the threshold to be 25%, and defined the area to be all pixels within distance 10 from at least one of the borders of the frame. We have chosen such a low threshold so to preserve many of the frames where a movement occurs on the edges while maintaining a dataset with little to no movement generated from a camera shift. For example, we maintained sequences in which people and objects enter and leave the frame. With this definition we moved to create the shots.

Another decision we made was to reduce the frames per second displayed in the shots. According to Carpenter [6], saccade latency is around 200ms. Therefore a frame rate of 5 per second seems appropriate. Additionally, in order for a mini-batch to be decent sized, we artificially demanded each shot to retain a minimum of 20 frames and a maximum of 32. Meanwhile, we also resized the frames to a less demanding 320x180 RGB channel. It seemed to be the middle ground between low resolution while conserving enough details for the model to learn.

The last significant cleaning effort we made was to clear the data from artificial objects, such as running captions or subtitles. Therefore many of our episodes do not include the shots taken right after the opening credits. Finally, the shots were sorted chronologically by season and episode from which they are taken in order to feed the agent in the correct order of events.

The final dataset consists of 203780 frames in 7855 shots of the television series The Big Bang Theory, each consisting of 20-32 frames of a video reduced to 5 frames per second 320x180 RGB channel. Furthermore we transformed the frames to 3 dimensional arrays of 32bits floating point numbers ranging from 0 to 1.

Table 1 shows the main parameters of the data. In this work, we split the data such that the training set contains the first 8 seasons and the validation and test set the last 2. It amounts to an 80/20 split with respect to seasons and a roughly the same (actually 82/18) with respect to the number of shots and number of total frames. As for the part of face detection, we split the Deep Curiosity Loop’s test set in 2. The validation set now consists of 24 shots, 1 from each episode of season 9. The rest goes to the test set.

4.2 Faces are Informative

Given this dataset, we can test our hypothesis that faces form the majority of the information channel, chosen to be represented by pixel-color difference. For this purpose, we extracted the squared

Table 1: Summary of dataset, 10 seasons of The Big Bang Theory.

Season	Number of Frames			Shots	Episodes
	mean	std	sum		
1	25.71	4.51	13.96K	543	17
2	26.03	4.52	19.86K	763	23
3	26.09	4.42	19.98K	766	23
4	26.12	4.42	24.48K	937	24
5	26.32	4.53	26.08K	991	24
6	26.03	4.48	21.84K	839	23
7	25.66	4.40	19.76K	770	24
8	25.87	4.45	21.70K	839	24
9	25.66	4.35	19.66K	766	24
10	25.68	4.45	16.46K	641	23
Total	25.94	4.46	203.78K	7855	229

difference images between all directly successive frames. Meanwhile we used an out of the box face detector from OpenCV (which uses a variant of Viola and Jones [36]) to obtain the locations of the faces in each image. Next we computed the distribution of the differences within the proposed locations for faces and outside of it. As can be seen in Fig. 2(inset), the mean squared change is significantly greater inside the region containing a face than outside of it ($Z = 1.86 \times 10^8$, $p < .0001$ Wilcoxon Signed-Ranks Test). This reflects our observation that this phenomenon was found to be correct in all but 3 pairs of successive frames.

This result shows that in general, larger rewards will come from pixels within the vicinity of a face than far from it. To put it differently, for a curious agent it is more interesting to look at a face than to look randomly anywhere else in the picture. However, other socially relevant features are prominent in the dataset, e.g. hands. Since we do not use labeled supervised learning, but curiosity-based learning, the resulting model cannot differentiate between different socially-relevant features and will mark faces as well as hands with high value, indiscriminately.

4.3 Socially-relevant Feature Detection

The simple learner we constructed Φ^L resulted in a straightforward convolution of a centered Gaussian (not shown). In other words, the learner converged to predicting the zero-th order of the visual dynamics, namely, the predicted next image is (almost) identical to the current image. This resulted in prediction errors that corresponded to movements or change within the video stream, as all static components are correctly predicted. Thus the reward matrix \mathbf{R} effectively represents changes in the scene. Taken together with the analysis of the dataset showing that faces are one of the major sources of change, we obtained a reward matrix corresponding to faces (and hands). We wish to emphasize that this was *not pre-programmed* or known a-priori, but rather is the emerging property of a simple CNN forward-model learner and the statistics of the embedding environment.

The link between rewards and faces and hands allow us to derive from the AC-DQN part of the Deep Curiosity Loop a set of socially-relevant feature detection models. We remind the reader that the Action-Convolution Deep-Q Network’s output is $\Phi^Q(I, A)$. However, contrary to previous variants of DQN, it is not a real-valued vector but a real-valued matrix with the width and height of I and depth the size of the action space (5 in this work).

4.3.1 Face and Hands Mask

Given an image I (Fig. 3(a)), we define the value image as $V(I) = \max_a \Phi^C(I, \hat{\mathbf{A}})$, Fig. 3(b). We now show that, as a result of our chosen environment, V can be used to form a face and hands detection model. To do so we generate a binary mask from it with respect to a given a threshold value t .

To test its worth as a face detector, we first picked a threshold by building a ROC curve (displayed in figure 2) from a validation set, where the ground truth is given by an OpenCV implementation of

Viola and Jones, the same algorithm with which we showed the existence of a face channel. We then measured the success of our detector by calculating Intersection Over Union (IOU) between it and our ground truth. The resulting AUC value of 0.877 shows that our unsupervised learned face detector works quite well. Further analysis on the test set re-confirms this result. However, it is important to note that since our model does not discriminate between faces and hands, a portion of the false negatives for face detection should still be considered as true positives for SFD.

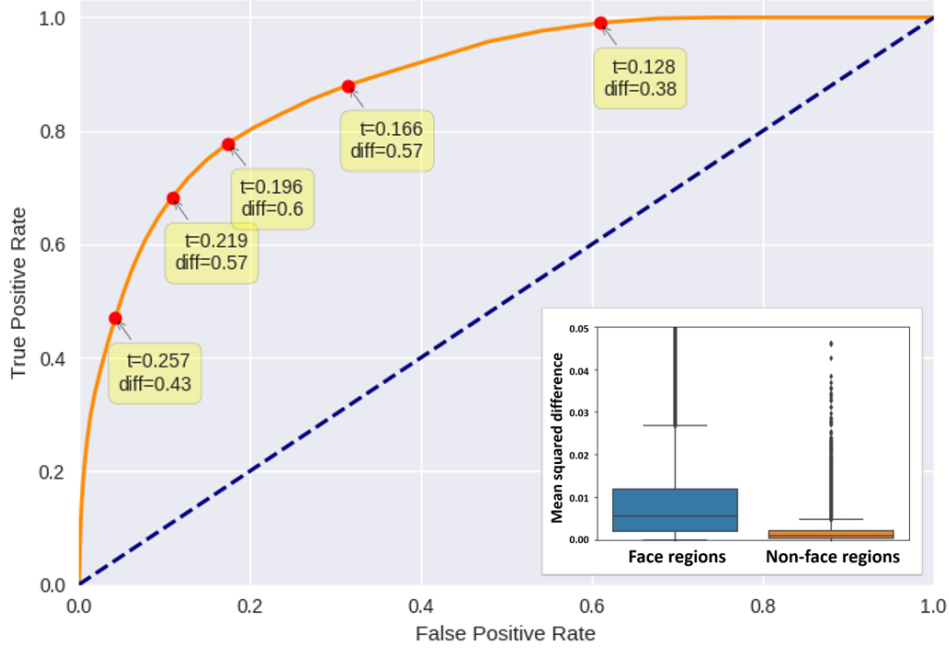


Figure 2: ROC curve of the value image, derived from the AC-DQN, with thresholds between -0.1 and 0.5. Inset: The mean squared difference between two successive frames, within a face region and outside of it. Cutoff at 0.05. A face region is detected using OpenCV frontal Viola-Jones face detector with 1.1 enlargement rate and with at least 6 neighbors. Performed on the first 6000 shots, only for frames where a face was detected, ≈ 100000 pairs

Threshold	FPR	TPR	Youden index
0.128	0.595343	0.993316	0.397973
0.166	0.310977	0.951039	0.640061
0.196	0.179516	0.861723	0.682208
0.219	0.113833	0.753707	0.639873

Table 2: Accuracy of four thresholds on the test set. We chose the Youden index as the optimality criteria, where it gives equal weight to the True Positive Rate (TPR) and the False Positive Rate (FPR) and is defined as $\max TPR - FPR$. We display the results of the 2 : 1 ratios, i.e. $\max (2 \cdot TPR - FPR)$ and $\max (TPR - 2 \cdot FPR)$.

4.3.2 Bounding Boxes

When it comes to face detection, most of the evaluation protocols rely on an output of a bounding box. Despite the fact that the DCL’s output is not of this form, we have augmented it with the following processes. First we resize the image to our model’s input dimensions (180×320). Next we find all local maxima of $V(I)$ that are not within 22 pixels from each other (22 because it is roughly half of the receptive field, which is 45 on each side) and produce a bounding box with each peak as the center of a 45×45 bounding box. Finally we translate those boxes to their location with respect to the original size of the image, Fig 3(a).

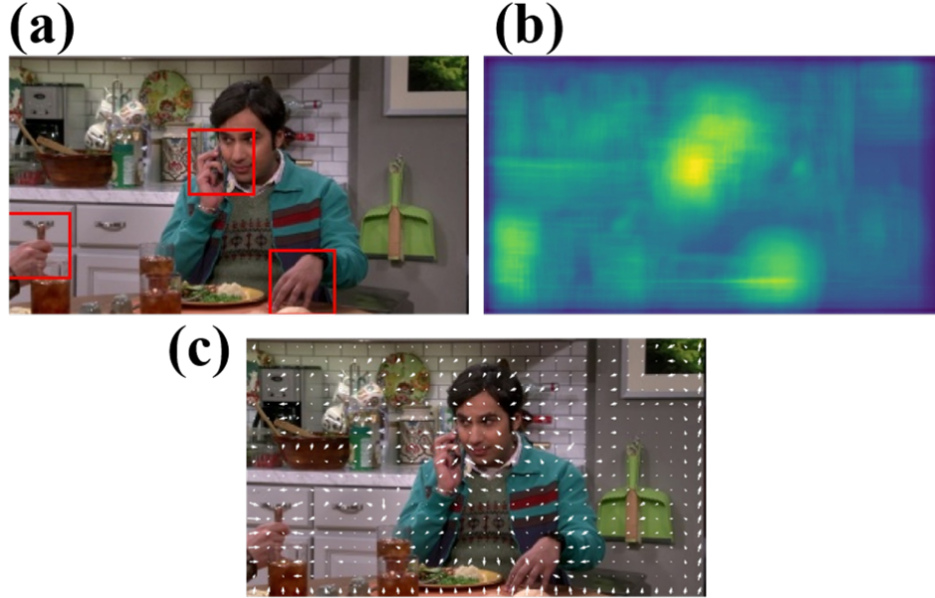


Figure 3: Examples of the output of the DCL architecture. (a) Input image with the resultant bounding boxes, I . (b) Value function $V(I)$. (c) Social Interaction Optical Flow, Φ^Q .

4.4 Social Interaction-Optical Flow

In addition to the SFD model, the policy $\pi(A | I)$ learned within the Deep Curiosity Loop provides a surrogate/closely related model. Learned via the novel Action-Convolution Deep-Q Network with the ϵ -greedy algorithm, it amounts to a “force field” applied on the image. This is the result of the “passive” nature of the action, i.e. movement is performed within the image, together with a one-to-one correspondence between states and pixels. As can be seen in figure Fig. 3(c) the field is pointing towards the faces and the hands. We call this field the Social Interaction Optical Flow.

5 Conclusions

Attempting to mimic infant’s learning processes and embedding environment, we developed a novel deep curiosity loop architecture. We have shown that faces are prominent motion sources within social scenes, hence, given a simplified forward model as a learner, results in rewarding faces. However, since our proposed framework corresponds to curiosity-based intrinsic motivation learning, it is not supplied with labels and learns the value of all socially relevant features. These are not restricted to faces but also include hands and objects relating to them, comparable to children’s normal visual development [7].

This lack of differentiation between faces and hands makes our model difficult to evaluate, since comparing to state-of-the-art face detectors [15] should not prove useful. A more comprehensive comparison to a fully labeled and segmented dataset, as used by Long et al. [22], could prove somewhat more adequate.

Our proposed framework is different from previous ones in several major aspects. Most notably, it attempts to learn *static* visual features from *dynamics* video feeds. Furthermore, utilizing the curiosity loop, training a value function does not require an external reward function or labels. Finally, while not mandatory, we have used online learning to better mimic infant’s learning processes and still arrived at a valuable model representing socially-relevant features.

Future work will extend our training model in two dimensions. The first will include many more social scenes, e.g. Glee and Silicon Valley, in order to increase the generalization aspects of our model. The second will replace normative social scenes with other more unique scenes, e.g. National Geographic, to explore which relevant features will emerge from the same framework. Finally,

deploying our proposed Deep Curiosity Loop architecture in a curious social robot might result in an infant-like learning process culminating in a socially engaging interaction.

References

- [1] A. G. Barto, S. Singh, and N. Chentanez. Intrinsically Motivated Learning of Hierarchical Collections of Skills. In *International Conference on Developmental Learning (ICDL)*, 2004.
- [2] Guy Ben-Yosef, Alon Yachin, and Shimon Ullman. A model for interpreting social interactions in local image regions. *arXiv preprint arXiv:1712.09299*, 2017.
- [3] Aleksandar Botev, Guy Lever, and David Barber. Nesterov’s Accelerated Gradient and Momentum as approximations to Regularised Update Descent. *arXiv:1607.01981 [cs, stat]*, July 2016. arXiv: 1607.01981.
- [4] Angela M. Brown. Development of visual sensitivity to light and color vision in human infants: A critical review. *Vision Research*, 30(8):1159–1188, January 1990. ISSN 0042-6989.
- [5] Angelo Cangelosi, Giorgio Metta, Gerhard Sagerer, Stefano Nolfi, Chrystopher Nehaniv, Kerstin Fischer, Jun Tani, Tony Belpaeme, Giulio Sandini, and Francesco Nori. Integration of action and language knowledge: A roadmap for developmental robotics. *Autonomous Mental Development, IEEE Transactions on*, 2(3):167–195, 2010. ISSN 1943-0604.
- [6] Roger HS Carpenter. *Movements of the Eyes, 2nd Rev.* Pion Limited, 1988.
- [7] Caitlin M. Fausey, Swapnaa Jayaraman, and Linda B. Smith. From faces to hands: Changing visual input in the first two years. *Cognition*, 152:101–107, July 2016.
- [8] B. Froba and A. Ernst. Face detection with the modified census transform. In *Sixth IEEE International Conference on Automatic Face and Gesture Recognition, 2004. Proceedings.*, pages 91–96, May 2004.
- [9] Goren Gordon and Ehud Ahissar. A Curious Emergence of Reaching. In *Advances in Autonomous Robotics*, Lecture Notes in Computer Science, pages 1–12. Springer, Berlin, Heidelberg, August 2012.
- [10] Goren Gordon and Ehud Ahissar. Hierarchical curiosity loops and active sensing. *Neural Networks*, 32 (Supplement C):119–129, August 2012.
- [11] Goren Gordon, Ehud Fonio, and Ehud Ahissar. Emergent Exploration via Novelty Management. *Journal of Neuroscience*, 34(38):12646–12661, 2014.
- [12] Goren Gordon, Ehud Fonio, and Ehud Ahissar. Learning and control of exploration primitives. *Journal of Computational Neuroscience*, 37(2):259–280, 2014.
- [13] Krisztina V. Jakobsen, Lindsey Umstead, and Elizabeth A. Simpson. Efficient human face detection in infancy. *Developmental Psychobiology*, 58(1):129–136, January 2016.
- [14] Swapnaa Jayaraman, Caitlin M. Fausey, and Linda B. Smith. The Faces in Infant-Perspective Scenes Change over the First Year of Life. *PLOS ONE*, 10(5):e0123780, May 2015. ISSN 1932-6203.
- [15] H. Jiang and E. Learned-Miller. Face Detection with the Faster R-CNN. In *2017 12th IEEE International Conference on Automatic Face Gesture Recognition (FG 2017)*, pages 650–657, May 2017. doi: 10.1109/FG.2017.82.
- [16] F. Kaplan and P. Y. Oudeyer. In search of the neural circuits of intrinsic motivation. *Frontiers in Neuroscience*, 1:11, 2007.
- [17] Diederik P. Kingma and Jimmy Ba. Adam: A Method for Stochastic Optimization. *arXiv:1412.6980 [cs]*, December 2014. arXiv: 1412.6980.
- [18] Varun Raj Kompella, Marijn Stollenga, Matthew Luciw, and Juergen Schmidhuber. Continual curiosity-driven skill acquisition from high-dimensional video inputs for humanoid robots. *Artificial Intelligence*, 2015. ISSN 0004-3702.
- [19] Q. V. Le. Building high-level features using large scale unsupervised learning. In *2013 IEEE International Conference on Acoustics, Speech and Signal Processing*, pages 8595–8598, May 2013.
- [20] Stan Z. Li, Long Zhu, ZhenQiu Zhang, Andrew Blake, HongJiang Zhang, and Harry Shum. Statistical Learning of Multi-view Face Detection. In *Proceedings of the 7th European Conference on Computer Vision-Part IV, ECCV ’02*, pages 67–81, London, UK, UK, 2002. Springer-Verlag.

- [21] D. Y. Little and F. T. Sommer. Learning and exploration in action-perception loops. *Front Neural Circuits*, 7:37, 2013.
- [22] Jonathan Long, Evan Shelhamer, and Trevor Darrell. Fully convolutional networks for semantic segmentation. In *Proceedings of the IEEE conference on computer vision and pattern recognition*, pages 3431–3440, 2015.
- [23] Clément Moulin-Frier and P-Y Oudeyer. Curiosity-driven phonetic learning. In *Development and Learning and Epigenetic Robotics (ICDL), 2012 IEEE International Conference on*, pages 1–8. IEEE, 2012. ISBN 1-4673-4964-X.
- [24] P. Y. Oudeyer, J. Gottlieb, and M. Lopes. Intrinsic motivation, curiosity, and learning. *Progress in Brain Research*, 229:257–284, January 2016.
- [25] Pierre-Yves Oudeyer, Frdric Kaplan, and Verena V. Hafner. Intrinsic motivation systems for autonomous mental development. *IEEE transactions on evolutionary computation*, 11(2):265–286, 2007.
- [26] S. Ren, K. He, R. Girshick, and J. Sun. Faster R-CNN: Towards Real-Time Object Detection with Region Proposal Networks. *IEEE Transactions on Pattern Analysis and Machine Intelligence*, 39(6):1137–1149, June 2017.
- [27] Tom Schaul, John Quan, Ioannis Antonoglou, and David Silver. Prioritized Experience Replay. *arXiv:1511.05952 [cs]*, November 2015. URL <http://arxiv.org/abs/1511.05952>. arXiv: 1511.05952.
- [28] J. Schmidhuber. *A possibility for implementing curiosity and boredom in model-building neural controllers*. MIT Press, 1990.
- [29] J. Schmidhuber. Curious model-building control systems. In *[Proceedings] 1991 IEEE International Joint Conference on Neural Networks*, pages 1458–1463 vol.2, November 1991.
- [30] J. Schmidhuber. Formal Theory of Creativity, Fun, and Intrinsic Motivation (1990-2010). *IEEE Transactions on Autonomous Mental Development*, 2(3):230–247, 2010.
- [31] Ozgur Simsek and Andrew G. Barto. *An intrinsic reward mechanism for efficient exploration*. ACM, 2006.
- [32] S. Singh, R. L. Lewis, A. G. Barto, and J. Sorg. Intrinsically Motivated Reinforcement Learning: An Evolutionary Perspective. *Autonomous Mental Development, IEEE Transactions on*, 2(2):70–82, 2010. ISSN 1943-0604.
- [33] Freek Stulp and Pierre-Yves Oudeyer. Emergent proximo-distal maturation through adaptive exploration. In *Development and Learning and Epigenetic Robotics (ICDL), 2012 IEEE International Conference on*, pages 1–6. IEEE, 2012.
- [34] R. S. Sutton and A. G. Barto. *Reinforcement learning : an introduction*. Adaptive computation and machine learning. MIT Press, Cambridge, Mass., 1998. ISBN 0262193981 (alk. paper).
- [35] Dmitry Ulyanov, Andrea Vedaldi, and Victor Lempitsky. Instance Normalization: The Missing Ingredient for Fast Stylization. *arXiv:1607.08022 [cs]*, July 2016. arXiv: 1607.08022.
- [36] P. Viola and M. Jones. Rapid object detection using a boosted cascade of simple features. In *Proceedings of the 2001 IEEE Computer Society Conference on Computer Vision and Pattern Recognition. CVPR 2001*, volume 1, pages I–511–I–518 vol.1, 2001.
- [37] Paul Viola and Michael J. Jones. Robust Real-Time Face Detection. *International Journal of Computer Vision*, 57(2):137–154, May 2004.
- [38] Paul Viola, Michael J. Jones, and Daniel Snow. Detecting Pedestrians Using Patterns of Motion and Appearance. *International Journal of Computer Vision*, 63(2):153–161, July 2005.
- [39] T. Walther and R. P. Würtz. Unsupervised learning of face detection models from unlabeled image streams. In *2012 BIOSIG - Proceedings of the International Conference of Biometrics Special Interest Group (BIOSIG)*, pages 1–11, September 2012.
- [40] J. Weng. Developmental Robotics: Theory and Experiments. *International Journal of Humanoid Robotics*, 1(2):199–236, 2004.
- [41] Shengye Yan, Shiguang Shan, Xilin Chen, and Wen Gao. Locally Assembled Binary (LAB) feature with feature-centric cascade for fast and accurate face detection. In *2008 IEEE Conference on Computer Vision and Pattern Recognition*, pages 1–7, June 2008.